

# Robust Constrained Model Predictive Control of Fast Electromechanical Systems

Franco Blanchini<sup>a</sup>, Daniele Casagrande<sup>b</sup>, Giulia Giordano<sup>a</sup>, Umberto Viaro<sup>b</sup>

<sup>a</sup>*Department of Mathematics and Computer Science, University of Udine, via delle Scienze 206,  
33100 Udine, Italy*

<sup>b</sup>*Polytechnic Department of Engineering and Architecture, University of Udine, via delle Scienze  
206, 33100 Udine, Italy*

---

## Abstract

A major drawback hinders the application of Model Predictive Control (MPC) to the regulation of electromechanical systems or, more generally, systems with fast dynamics: the time needed for the online computation of the control is often too long with respect to the sampling time. This paper shows how this problem can be overcome by suitably implementing the MPC technique. The main idea is to compute the control law using the discrete-time Euler Auxiliary System (EAS) associated with the continuous-time plant, and apply the control obtained for the discrete-time system to the continuous-time system. In this way the implementation sampling time can be much smaller than the EAS time parameter, which leads to significant savings in computation time. Theoretical results guarantee stabilisation, constraint satisfaction and robustness of such a control strategy, which is applied to the control of an electric drive and a cart-pendulum system.

*Keywords:* Model Predictive Control, Euler Auxiliary System, Constrained Control, Stability, Permanent-Magnet Motor Drive, Cart-Pendulum System

---

## 1. Introduction

Model Predictive Control (MPC), also referred to as Receding Horizon Control, is an established control technique (see, for instance, [9]) that was initially intended for linear time-invariant (LTI) systems. Despite the heavy computational

---

*Email addresses:* blanchini@uniud.it (Franco Blanchini),  
daniele.casagrande@uniud.it (Daniele Casagrande),  
giulia.giordano@uniud.it (Giulia Giordano), viaro@uniud.it (Umberto Viaro)

burden required by its implementation, MPC is characterised by a high level of robustness, which has motivated its extension to other important classes of systems, such as distributed systems [10, 11] and nonlinear systems [20]. Its application in industrial contexts is more recent (see, e.g., [21]).

In the last years the MPC technique has been applied to the control of electric equipment, such as power converters [22, 1, 29] and electromechanical systems with fast dynamics [24, 28], with particular regard to electric drives [12, 13, 8, 18]. An overview of results on this subject can be found in [16] and [23].

The industrial application of the MPC technique to the regulation of the aforementioned systems has a severe drawback: the time needed for its real-time implementation is often too long. Several methods have been proposed to overcome this problem. Some of them are based on the idea of performing off-line part of the computation needed to find a solution (see, e.g. [26, 2, 17]). Some others, instead, aim at speeding up computations. For instance, an interesting solution that combines *warm-starting*, reordering of the variables and *early termination* is proposed in [27]. Another approach is followed in [3], where the state space is divided into subsets that require the solution of simpler linear quadratic problems. However, in general, there is no upper bound on the number of these subsets, which may grow exponentially with the dimension of the prediction horizon. Other solutions, such as the so-called Generalized Predictive Control [15] and Finite Control Set MPC [16], have also been investigated.

Here we pursue the idea of quasi-optimal MPC put forth in [6], which is summarised in Section 2. The key feature of the method is to consider the Euler Auxiliary System (EAS) for the computation of the MPC law. In fact, the control law determined by means of the MPC technique for the *discrete-time* EAS can safely be applied to the *continuous-time* system. In this way, the implementation sampling time can be made much smaller than the time parameter adopted in the sampled-data prediction model, with remarkable computational benefits. Section 3 analyses the robustness of the suggested technique. In particular, a condition is derived that ensures robust stability in the presence of parametric uncertainties. The effectiveness of the method is tested on two fast electromechanical systems. Specifically, Section 4 considers the control of a permanent-magnet synchronous motor, while Section 5 deals with a cart-pendulum system. The results are briefly discussed in the concluding Section 6.

## 2. MPC strategy

### 2.1. Motivation and background

MPC techniques based on standard sampled-data models must satisfy the following requirements that are often conflicting.

- The sampling time must be small; roughly, the sampling frequency must be significantly greater than the system bandwidth.
- The prediction horizon must be large enough to allow an effective optimisation of the trajectory.
- The time required to compute the solution must be smaller than the sampling time.

Unfortunately, both reducing the sampling time and extending the prediction horizon increase the number of variables in the optimisation problem that must be solved to find the control law, which results in a longer computation time. Coping with these conflicting requirements is even harder in the presence of constraints.

The idea suggested in [6] and applied in this paper is to distinguish between two different time intervals:

$T$ : the *implementation sampling time*, which is chosen on the basis of the system bandwidth and must be small enough to cope with the fast system dynamics.

$\tau$ : the *time parameter* adopted in the prediction model. This parameter is chosen on the basis of the prediction horizon and must be large enough to ensure that the solution of the optimisation problem is computed within time  $T$ .

In short,

$$\tau \gg T .$$

Now, if  $T$  is very small (virtually zero w.r.t. the process time constants), the sampled-data implementation is virtually equivalent to a continuous-time implementation and the following questions arise.

Q1 How can an MPC scheme based on the time parameter  $\tau$  be adopted and applied to the continuous-time system?

Q2 What performance can be guaranteed?

Q3 Can constraint satisfaction be ensured?

The next subsection answers these questions.

## 2.2. Overview of constrained suboptimal MPC [6]

Consider a system

$$\dot{x}(t) = f(x(t), u(t)), \quad (1)$$

where  $x(t) \in \mathbb{R}^n$  for all  $t$ ,  $u(t) \in \mathbb{R}^m$  for all  $t$ , and  $f(\cdot, \cdot)$  is locally Lipschitz with respect to the first argument. Assume that  $\bar{x} = 0$  is an equilibrium point corresponding to  $\bar{u} = 0$ , namely  $f(0, 0) = 0$ , and denote the initial state by  $x_0 = x(0)$ . We are concerned with the problem of finding the control law  $u$  that minimises the cost functional

$$J(x, u) = \int_0^\infty g(x(t), u(t)) dt, \quad (2)$$

where  $g$  is positive definite, subject to the constraints

$$x(t) \in \mathcal{X} \quad (3)$$

$$u(t) \in \mathcal{U} \quad (4)$$

for all  $t$ , where  $\mathcal{X}$  and  $\mathcal{U}$  are convex and closed sets including the origin in their interior.

Now, suppose that the optimal control law minimising the cost functional and satisfying the constraints can be written in the state-feedback form

$$u(t) = K_{opt}(x(t)). \quad (5)$$

If the optimal cost is finite and  $K_{opt}$  is well-defined, we can consider the cost-to-go function

$$\Psi(x_0) \doteq J(x, K_{opt}(x)) = \int_0^\infty g(x(t), K_{opt}(x(t))) dt, \quad (6)$$

with

$$\dot{x}(t) = f(x(t), K_{opt}(x(t))), \quad x(0) = x_0, \quad (7)$$

which represents the value of the optimal cost, subject to the constraints, given the initial state  $x_0$ .

Since, except for special cases, finding  $K_{opt}$  and  $\Psi$  is an almost hopeless task, resort can profitably be made to the EAS

$$x(k+1) = x(k) + \tau f(x(k), u_D(k)), \quad (8)$$

where  $\tau > 0$  is the aforementioned *time parameter*, and to the associated cost function

$$J_D^\tau(x, u) = \tau \sum_{k=0}^{\infty} g(x(k), u_D(k)). \quad (9)$$

If, as previously assumed, the discrete-time optimal control may be expressed in the state-feedback form  $u_D(k) = K_D(x(k))$ , the EAS dynamics can be written as

$$x(k+1) = x(k) + \tau f(x(k), K_D(x(k))), \quad x(0) = x_0 \quad (10)$$

and the cost-to-go function  $\Psi_D(x_0, \tau)$ , i.e., the optimal discrete-time cost with initial state  $x_0$  subject to the given constraints, is

$$\Psi_D(x_0, \tau) \doteq J_D^r(x, K_D(x)) = \tau \sum_{k=0}^{\infty} g(x(k), K_D(x(k))). \quad (11)$$

The following result, proven in [6], points out an important relation between the continuous-time problem and the discrete-time solution.

**Theorem 2.1.** *Assume that  $\Psi_D$  and  $\Psi$  are convex functions defined on an open convex set including the origin. Then, for all  $\tau > 0$ ,*

$$\Psi(x_0) \leq \Psi_D(x_0, \tau).$$

*Moreover, if the control  $K_D(x)$  is applied to the continuous-time system, the continuous-time cost (2) with initial state  $x(0) = x_0$  is bounded as*

$$J(x, K_D(x)) \leq \Psi_D(x_0, \tau)$$

*and, for  $\tau \rightarrow 0^+$ ,  $\Psi_D(x_0, \tau)$  converges to  $\Psi(x_0)$  from above.* □

If the system is linear time-invariant, i.e.,

$$\dot{x}(t) = Ax(t) + Bu(t), \quad (12)$$

then the corresponding EAS is

$$x(k+1) = [I + \tau A]x(k) + \tau Bu_D(k). \quad (13)$$

It can be shown [6] that, if the pair  $(A, B)$  is stabilisable and the function  $g$  is convex, then  $\Psi(\cdot)$  and  $\Psi_D(\cdot, \tau)$ ,  $\forall \tau$ , are both convex functions defined on an open convex set including the origin. Hence, in view of Theorem 2.1, the discrete-time feedback control  $K_D(x)$  can be reasonably applied to the continuous-time system (12).

Consider now the MPC problem

$$\Psi_N^{(\tau)}(x_0) = \min_{u_D(\cdot), x(\cdot)} \left[ \tau \sum_{k=0}^{N-1} g(x(k), u_D(k)) + \Phi(x(N)) \right], \quad (14)$$

subject to

$$x(k+1) = [I + \tau A]x(k) + \tau B u_D(k), \quad 0 \leq k \leq N-1, \quad (15)$$

$$u_D(k) \in \mathcal{U}, \quad 0 \leq k \leq N-1, \quad (16)$$

$$x(k) \in \mathcal{X}, \quad 0 \leq k \leq N-1, \quad (17)$$

$$x(0) = x_0, \quad (18)$$

$$x(N) \in \mathcal{P}, \quad (19)$$

where  $N$  is the number of steps in the prediction horizon and  $\Phi(x(N))$  is a penalisation of the final state  $x(N)$  (included to enforce system stability). The constraint (19) on the final state  $x(N)$ , where  $\mathcal{P}$  is a controlled-invariant set (or a contractive set [4, 5]), is also considered.

Based on the solution of the discrete-time problem (14)–(19), a control law for the continuous-time linear system (12) providing an approximate solution to the problem of minimising the finite-horizon cost functional (2), *with a guaranteed cost*  $J \leq \Psi_N^{(\tau)}(x_0)$ , can be computed according to the following procedure.

**Procedure 2.1. Continuous-time control law.**

**Step 1** *Given the state  $x(t)$  of the continuous-time system at time  $t = kT$ ,  $k = 0, 1, 2, \dots$ , find the control sequence*

$$\{u_D(0), u_D(1), \dots, u_D(N-1)\}$$

*that solves the discrete-time optimisation problem (14)–(19) starting from  $x_0 = x(t)$ .*

**Step 2** *Apply to the original continuous-time system the control input  $u(t) = u_D(0)$  (first element of the discrete-time optimal control sequence) for all  $t \in [kT, (k+1)T)$ .*

**Remark 2.1.** *In practice, the computation of the values of the piecewise-constant control law takes a non-zero time, so that over a short subinterval at the beginning of every sampling interval the input value will remain the same as that in the preceding sampling interval.*

If

$$g(x, u) = x^\top Qx + u^\top Su, \quad (20)$$

where  $Q$  and  $S$  are positive-definite matrices, then the optimal *unconstrained* cost is

$$\Psi(x_0) = \tau x_0^\top P x_0,$$

where  $P$  is the solution of the discrete-time algebraic Riccati equation associated with (13), and  $\Psi_N^{(\tau)}(x_0)$  provides the *true constrained discrete-time optimal cost* for the EAS, provided that the horizon  $N$  is large enough [25, 19, 14].

Since  $\Psi_N^{(\tau)}$  is convex (actually, piecewise-quadratic [3]), when the piecewise-constant control computed by means of Procedure 2.1 is applied to the continuous-time system, the constraints are satisfied and the continuous-time cost is bounded from above by the discrete-time cost  $\Psi_N^{(\tau)}(x_0)$  according to the following result [6] that ensures stability, too.

**Theorem 2.2.** *Let  $u = K_D(x)$  be the continuous-time control law determined by means of Procedure 2.1. Then, for  $N$  large enough,*

- *no constraint violation occurs for the continuous-time system, and*
- *$\Psi_N^{(\tau)}$  is a Lyapunov function for the continuous-time system satisfying the inequality*

$$D^+ \Psi_N^{(\tau)}(x) \leq -\phi(x), \quad (21)$$

*where  $D^+ \Psi_N^{(\tau)}$  denotes the right Lyapunov derivative<sup>1</sup> of  $\Psi_N^{(\tau)}$  and  $\phi$  is a positive-definite function.*

**Proof.** (Sketch - for a detailed proof, see [6].) According to [25, 19, 14], if the horizon  $N$  is large enough,  $\Psi_N^{(\tau)}$  is a Lyapunov function for the discrete-time EAS. As a consequence, there exists a positive definite function  $\phi_D$ , such that

$$\Psi_N^{(\tau)}(x + \tau(Ax + BK_D(x))) - \Psi_N^{(\tau)}(x) \leq -\phi_D(x). \quad (22)$$

---

<sup>1</sup>It is necessary to consider the *right Lyapunov derivative*, defined as  $D^+ \Psi(x) = \lim_{h \rightarrow 0^+} \frac{\Psi(x(t+h)) - \Psi(x(t))}{h}$ , because  $\Psi$  is convex but, in general, non-smooth.

By setting

$$\phi(x) := \phi_D(x)/\tau,$$

from (22) we obtain

$$\frac{\Psi_N^{(\tau)}(x + \tau(Ax + BK_D(x))) - \Psi_N^{(\tau)}(x)}{\tau} \leq -\phi(x). \quad (23)$$

If  $\Psi_N^{(\tau)}$  is convex, its right Lyapunov derivative can be written as the limit for  $\tau \rightarrow 0^+$  of the left-hand side of (23), which is a non-decreasing function of  $\tau$  and, consequently,

$$\begin{aligned} D^+ \Psi_N^{(\tau)}(x) &= \lim_{h \rightarrow 0^+} \frac{\Psi_N^{(\tau)}(x + h(Ax + BK_D(x))) - \Psi_N^{(\tau)}(x)}{h} \\ &\leq \frac{\Psi_N^{(\tau)}(x + \tau(Ax + BK_D(x))) - \Psi_N^{(\tau)}(x)}{\tau} \leq -\phi(x). \end{aligned}$$

■

### 3. Robustness of the control strategy

A theoretical result with important practical implications on the robustness of the proposed control strategy is derived in this section.

The theory presented in the previous section applies as long as  $\Psi_N^{(\tau)}$  is convex, which is certainly true in the case of linear systems with convex constraints. If the system is nonlinear, resort can be made to linearisation. Two types of linearisation are possible:

- *linearisation* around an equilibrium point, obtained by Taylor-expansion truncation;
- *feedback linearisation*, obtained by applying a suitable feedback to the non-linear system.

In both cases, the resulting model exhibits uncertainties: in the first, because the higher-order nonlinear terms are neglected; in the latter, because exact cancellation is impossible if the parameter values are not known precisely. Therefore, a realistic use of the model should take into account parameter uncertainties. It is shown next by means of a Lyapunov approach that, under suitable assumptions, the robustness of the adopted solution is guaranteed.

Consider the system

$$\dot{x}(t) = [A + \Delta] x(t) + Bu(t), \quad (24)$$

where matrix  $\Delta$ , which represents the uncertainty on the state matrix  $A$  and can itself be a function of the current state, i.e.,  $\Delta = \Delta(x)$  (for simplicity, only the state matrix  $A$  is assumed to be uncertain), satisfies a bound

$$\|\Delta(x)\| \leq \mu. \quad (25)$$

for all  $x$ . Then, the following result holds.

**Proposition 1.** *Assume that the nominal system (12) with  $u = K_D(x)$  admits the Lyapunov function  $\Psi_N^{(\tau)}$ , whose right Lyapunov derivative satisfies (21). Then, the stability of the uncertain system (24) is ensured if*

$$\psi(x) < \phi(x) \quad (26)$$

for all  $x$ , where

$$\psi(x) = \lim_{h \rightarrow 0^+} \frac{\Psi_N^{(\tau)}(x + h\Delta(x)x) - \Psi_N^{(\tau)}(x)}{h}. \quad (27)$$

**Proof.** It is enough to prove that  $\Psi_N^{(\tau)}$  is a Lyapunov function for the uncertain system (24). Indeed, if  $\Psi_N^{(\tau)}$  is differentiable at all points, then, denoting by  $\nabla \Psi_N^{(\tau)}$  its gradient, from (21) and (24) we have

$$\begin{aligned} D^+ \Psi_N^{(\tau)}(x) &= \nabla \Psi_N^{(\tau)}(x)^\top [Ax + \Delta(x)x + BK_D(x)] \\ &= \nabla \Psi_N^{(\tau)}(x)^\top [Ax + BK_D(x)] + \nabla \Psi_N^{(\tau)}(x)^\top \Delta(x)x \\ &\leq -\phi(x) + \psi(x) < 0. \end{aligned}$$

In general, however,  $\Psi_N^{(\tau)}$  is not differentiable at all points (for example, in the constrained linear-quadratic case it is piecewise quadratic [3]). The proof for the general case is given in the Appendix.  $\blacksquare$

To exploit this result, it is necessary to check whether condition (26) is satisfied for some positive-definite function  $\phi(x)$ . Now, if a Lipschitz constant  $c_L$  for  $\Psi_N^{(\tau)}$  in a certain domain  $\mathcal{X}_L \in \mathcal{X}$  is known, then from (25) and (27) we have

$$\psi(x) \leq c_L \mu \|x\|,$$

for all  $x \in \mathcal{X}_L$ . Another bound can be obtained if  $\phi(x) \leq \alpha \|x\|^2$ ; in this case

$$\psi(x) \leq \alpha \mu^2 \|x\|^2.$$

An explicit robustness condition valid when the constraints are not active<sup>2</sup> can also be found. Indeed, as far as the linear-quadratic *constrained* control problem [14, 19] is concerned, it is always possible to find a neighbourhood  $\mathcal{X}$  of the origin such that, for all initial conditions  $x_0 \in \mathcal{X}$ ,  $\Psi_N^{(\tau)}(x_0) = \tau x_0^\top P x_0$ , where  $P$  is the positive-definite solution of the discrete-time algebraic Riccati equation associated with the EAS (13). In this case, according to [14, p. 264],  $\phi_D$  in (22) can be chosen as  $\phi_D(x) = \tau x^\top Q x$  so that  $\phi(x) = x^\top Q x$  and, therefore, according to condition (21) of Theorem 2.2, the following relation holds for the nominal system

$$\dot{\Psi}_N^{(\tau)}(x) = \tau (Ax + BK_D(x))^\top P x + \tau x^\top P (Ax + BK_D(x)) \leq -x^\top Q x.$$

To guarantee robustness, the extra term  $\Delta(x)x$  accounting for the uncertainties must be added to the expression of the derivative  $\dot{\Psi}_N^{(\tau)}(x)$ , which leads, in the case of the uncertain system, to:

$$\begin{aligned} \dot{\Psi}_N^{(\tau)}(x) &= \tau [(A + \Delta(x))x + BK_D(x)]^\top P x + \tau x^\top P [(A + \Delta(x))x + BK_D(x)] \\ &\leq -x^\top Q x + \tau x^\top (\Delta(x)^\top P + P \Delta(x)) x \end{aligned}$$

and the condition to be checked becomes

$$x^\top Q x > \tau x^\top [\Delta(x)^\top P + P \Delta(x)] x. \quad (28)$$

This is certainly true if  $x^\top Q x > 2\tau \|P\| \|\Delta(x)\| \|x\|^2$  for all  $x$ , which in turn is satisfied if

$$\sigma_{\min}(Q) > 2\mu\tau \|P\|, \quad (29)$$

where  $\sigma_{\min}(Q)$  is the minimum eigenvalue of  $Q$ .

**Remark 3.1.** *Condition (29) might be satisfied only for small values of  $\mu$ . However, if the uncertain term  $\Delta(x)$  belongs to some known set  $\mathcal{D}$  for all  $x$ , to fulfill (28) it is sufficient that the eigenvalues of  $\Delta(x)^\top P + P \Delta(x) - Q$  be negative for all  $\Delta(x) \in \mathcal{D}$ . This remark is exploited at the end of the next section to determine the robustness margin of the control law.*

In the next two sections, the suggested MPC strategy is applied to a pair of fast electromechanical systems that are widely used in practice.

---

<sup>2</sup>We remind that the constraint  $x \in \mathcal{X}$  is *active* at  $\hat{x}$  if  $\hat{x}$  belongs to the boundary of  $\mathcal{X}$ .

#### 4. Permanent-magnet motor drive

The dynamics of a permanent-magnet synchronous motor can be described [7, 8] by the equations

$$\begin{aligned}\frac{di_d}{dt} &= \frac{1}{L_d}(-Ri_d + \omega L_q i_q + u_d), \\ \frac{di_q}{dt} &= \frac{1}{L_q}(-\omega L_d i_d - Ri_q - \omega M + u_q),\end{aligned}\tag{30}$$

where  $i_d$  and  $i_q$  are the direct and quadrature stator currents, respectively;  $R$  is the stator resistance;  $L_d$  and  $L_q$  are the direct and quadrature inductances;  $\omega$  is the rotor angular velocity;  $M$  is the permanent-magnet flux linkage;  $u_d$  and  $u_q$  are the direct and quadrature stator voltages.

Since  $\omega$  is measurable and  $M$  is known, reference can be made to a new variable  $\tilde{u}_q$  related to the quadrature voltage by

$$u_q = \tilde{u}_q + \omega M.$$

Then, by setting  $\mathbf{y} = (i_d, i_q)^\top$  and  $\mathbf{u} = (u_d, \tilde{u}_q)^\top$ , system (30) can be rewritten in the compact form

$$\dot{\mathbf{y}} = (\omega\Lambda - \Gamma)\mathbf{y} + \Theta\mathbf{u},\tag{31}$$

where

$$\Gamma = \begin{bmatrix} R/L_d & 0 \\ 0 & R/L_q \end{bmatrix}, \quad \Lambda = \begin{bmatrix} 0 & L_q/L_d \\ -L_d/L_q & 0 \end{bmatrix}$$

and

$$\Theta = \begin{bmatrix} 1/L_d & 0 \\ 0 & 1/L_q \end{bmatrix}.$$

The dynamics of the shaft angular speed are described by

$$\frac{d\omega}{dt} = \frac{p}{J_I} \left( \frac{3pM}{2} i_q - \frac{b}{p} \omega - \tau_L \right),\tag{32}$$

where  $p$  is the number of pole pairs,  $J_I$  is the moment of inertia,  $b$  is the viscous damping coefficient and  $\tau_L$  is the disturbance torque.

Suppose now that the equilibrium point  $\bar{\mathbf{y}}$  of (31) corresponding to a constant input vector  $\bar{\mathbf{u}}$  must be stabilised, and consider the state error

$$\mathbf{z} = \mathbf{y} - \bar{\mathbf{y}},$$

whose dynamics are described by

$$\dot{\mathbf{z}} = (\bar{\omega}\Lambda - \Gamma)\mathbf{z} + (\omega - \bar{\omega})\Lambda\mathbf{y} + \Theta(\mathbf{u} - \bar{\mathbf{u}}), \quad (33)$$

where  $\bar{\omega}$  is the equilibrium value for  $\omega$ . By applying the feedback control law

$$\mathbf{u} = \bar{\mathbf{u}} - \Theta^{-1}(\omega - \bar{\omega})\Lambda\mathbf{y} + \Theta^{-1}\mathbf{v}, \quad (34)$$

where  $\mathbf{v} = (v_d, v_q)^\top$  is a new input vector, the following linear equation is obtained

$$\dot{\mathbf{z}} = (\bar{\omega}\Lambda - \Gamma)\mathbf{z} + \mathbf{v}. \quad (35)$$

Concerning the angular velocity, at steady state from (32) we have

$$0 = \frac{p}{J_I} \left( \frac{3pM}{2} \bar{i}_q - \frac{b}{p} \bar{\omega} - \bar{\tau}_L \right), \quad (36)$$

where  $\bar{\tau}_L = 0$  is the nominal torque and  $\bar{\omega}$  the steady-state angular velocity. Denoting by

$$\sigma = \omega - \bar{\omega} \quad (37)$$

the deviation of the angular speed from its steady-state value, the overall control system can then be described by means of the linear equations

$$\dot{\mathbf{z}} = (\bar{\omega}\Lambda - \Gamma)\mathbf{z} + \mathbf{v}, \quad (38)$$

$$\dot{\sigma} = \alpha z_q - \beta \sigma - \delta \tau_L, \quad (39)$$

where  $\alpha = \frac{3p^2M}{2J_I}$ ,  $\beta = \frac{b}{J_I}$  and  $\delta = \frac{p}{J_I}$ .

An even simpler linear model can be obtained by setting

$$\mathbf{u} = \mathbf{v} - \Theta^{-1}(\omega\Lambda - \Gamma)\mathbf{y} \quad (40)$$

directly in (31), which leads to the state-error equation

$$\dot{\mathbf{z}} = \mathbf{v} \quad (41)$$

instead of (38).

The MPC strategy can conveniently be computed for either of the aforementioned linear models, which are exactly equivalent to the original system as long as the parameters are known accurately (i.e.,  $\omega$ ,  $i_d$ ,  $i_q$  can be measured precisely

and the information about the values of  $M$ ,  $L_d$  and  $L_q$  is reliable), so that replacing (34) in (33), or (40) in (31), leads to a perfect “cancellation” of the nonlinear terms. Quite arbitrarily, the simulations described next use the second model, whereas the robustness analysis at the end of the section is based on the first.

As in [8, 7], the limits  $|i_q| \leq i_{max}$  and  $|i_d| \leq \varepsilon i_{max}$ , with  $\varepsilon \in (0, 1)$ , are imposed on the quadrature and direct current, respectively, which is equivalent to imposing the following constraints on the components of  $\mathbf{z} = (z_d, z_q)^\top$ :

$$\begin{aligned} -\varepsilon i_{max} - \bar{i}_d &\leq z_d \leq \varepsilon i_{max} - \bar{i}_d, \\ -i_{max} - \bar{i}_q &\leq z_q \leq i_{max} - \bar{i}_q. \end{aligned}$$

The optimal control is computed with respect to the index

$$J(\mathbf{z}, \sigma, \mathbf{v}) = \int_0^\infty [\|\mathbf{z}(t)\|^2 + 10 \sigma(t)^2 + 0.01 \|\mathbf{v}(t)\|^2] dt. \quad (42)$$

The values of the parameters used in the numerical simulations are taken from [8]; precisely:

$$\begin{aligned} R &= 0.8 \, \Omega, \\ L_d &= 6.5 \, mH, \\ L_q &= 6.5 \, mH, \\ b &= 0.01 \, kg \cdot m^2/s, \\ M &= 0.36 \, Wb, \\ J_I &= 0.0085 \, kg \cdot m^2, \\ p &= 3, \\ i_{max} &= 10A, \\ \varepsilon &= 0.1. \end{aligned}$$

Since the speed transients are expected to last about  $0.1 \div 0.3 \, s$ , the prediction horizon is taken to be

$$T_{pred} = 0.3 \, s.$$

Considering the time-scale of this system, a reasonable sampling time is

$$T = 0.001 \, s,$$

so that the prediction horizon with  $\tau = T$  would include  $N = 300$  steps. Correspondingly, the optimisation problem, to be solved in a time *at most equal to*  $T$ ,

would involve about  $5 \cdot 300 = 1500$  free variables! Instead, the EAS with time parameter

$$\tau = 0.05 \text{ s},$$

consists of only  $N = 6$  steps leading to  $5 \cdot 6 = 30$  free variables, so that the optimisation problem can safely be solved within the sampling time.

In the simulations whose results are shown in Figs. 1 and 2, the reference speed is a square wave with high value  $1500 \text{ rpm}$ , low value  $500 \text{ rpm}$ , period  $2 \text{ s}$  and duty-cycle  $50\%$ . The load is due solely to the viscous torque term  $b\omega$ , while the disturbance torque is neglected. Fig. 1 shows the evolution of the state variables (currents and speed) and Fig. 2 that of the corresponding control inputs (voltages).

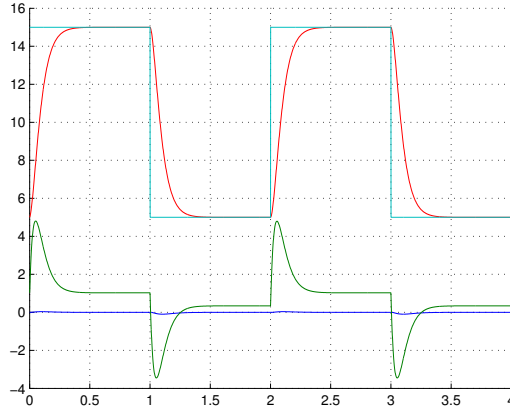


Figure 1: Evolution of the state variables: angular velocity (red) in  $\text{rpm}/100$  (for comparison, the reference signal is drawn in cyan), direct current (blue) and quadrature current (green) ( $A$ ).

According to the considerations of Section 3, the robustness of the suggested MPC technique can be evaluated as follows. It is assumed, for simplicity, that the only uncertain parameter is the stator resistance (which is often the case in practice). To this purpose, matrix  $\Gamma$  defined immediately after equation (31) is replaced by  $(1 + \gamma)\Gamma$  with  $\gamma$  positive (the resistance is higher than the nominal one during operation because of increased temperature). In this way, with reference to the system (38)–(39) with state vector  $\mathbf{x} = (\mathbf{z}^\top, \sigma)^\top$ , the uncertainty matrix  $\Delta$  in (24) takes the form

$$\Delta = -\gamma \begin{bmatrix} \Gamma & 0 \\ 0 & 0 \end{bmatrix}.$$

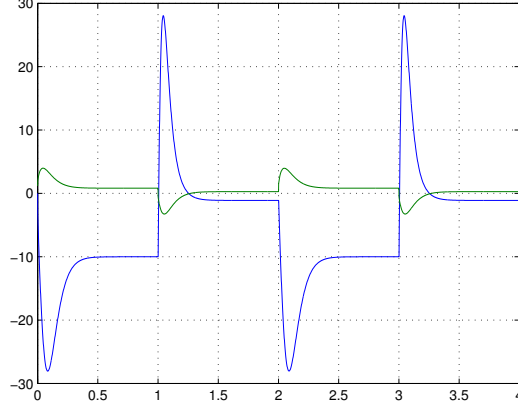


Figure 2: Evolution of the control inputs: direct voltage (blue) and quadrature voltage (green) (V).

Therefore, condition (28) particularises to

$$x^\top Q x > -\tau x^\top \gamma (\hat{\Gamma} P + P \hat{\Gamma}) x, \quad (43)$$

where

$$\hat{\Gamma} = \begin{bmatrix} \Gamma & 0 \\ 0 & 0 \end{bmatrix}$$

and  $P$  is the solution of the Riccati equation computed for the associated discrete-time EAS. Simple calculations show that (43) is satisfied for values of  $\gamma$  up to 0.35, corresponding to a 35% robustness margin.

## 5. Cart-pendulum system

Consider the cart-pendulum system of Fig. 3 actuated by means of a DC motor. By choosing the state vector as  $\mathbf{x} = [\vartheta \ \dot{\vartheta} \ s \ \dot{s}]^\top$ , the input  $u$  as the cart acceleration (directly related to the actuator torque which is approximately proportional to the armature current), and the output vector as  $\mathbf{y} = [\vartheta \ s]^\top$ , the linearised system equations can be written as

$$\begin{aligned} \dot{\mathbf{x}}(t) &= A\mathbf{x}(t) + B u(t), \\ \mathbf{y}(t) &= C\mathbf{x}(t). \end{aligned}$$

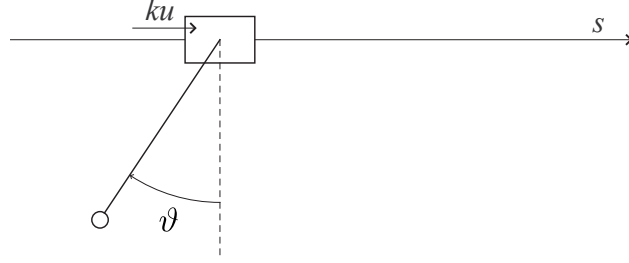


Figure 3: Cart-pendulum system.

The entries of the state, input and output matrices have been determined (in SI units) from a laboratory prototype as

$$A = \begin{bmatrix} 0 & 1 & 0 & 0 \\ -19.62 & -0.125 & 0 & -9.886 \\ 0 & 0 & 0 & 1 \\ 0 & 0 & 0 & -4.943 \end{bmatrix}, \quad B = \begin{bmatrix} 0 \\ 11.53 \\ 0 \\ 5.767 \end{bmatrix},$$

$$C = \begin{bmatrix} 1 & 0 & 0 & 0 \\ 0 & 0 & 1 & 0 \end{bmatrix}.$$

The system is subject to the acceleration constraint

$$|u(t)| \leq u_{max} = 1$$

and the angle constraint

$$|\vartheta(t)| \leq \vartheta_{max} = 0.23.$$

Matrices  $Q$  and  $S$  in (20) are chosen as  $Q = \text{diag}\{1, 1, 100, 1\}$  and  $S = 0.01$ . Even if this system is slower than the electrical drive considered in the previous section, the sampling time must be small to allow for the reconstruction of both the linear and angular speed from the displacement and angle measurements. In this case, an acceptable sampling time is  $T = 0.01$  s and a reasonable planning horizon is 0.5-1 s corresponding to 50-100 time steps, which would entail about 250-500 variables in a standard MPC problem to be solved in less than 0.01 s!

Instead, the EAS with time parameter  $\tau = 0.2$  s consists, for a planning horizon of 0.8 s, of 4 steps. Fig. 4 shows the state trajectories with the proposed receding-horizon control strategy starting from the initial state  $\mathbf{x}_0 = [0 \ 0 \ 0.5 \ 0]^\top$ . Figs. 5 and 6 show the state trajectories, starting from the same initial condition, when the prediction horizon is  $N = 8$  (corresponding to  $T_{pred} = 1.2$  s) and  $N = 12$  (corresponding to  $T_{pred} = 2.4$  s), respectively.

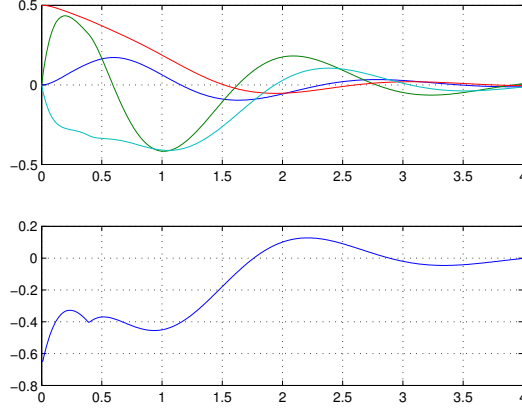


Figure 4: Simulation of the cart-pendulum behaviour starting from  $\mathbf{x}_0 = [0 \ 0 \ 0.5 \ 0]^\top$  for  $\tau = 0.2 \text{ s}$  and  $N = 4$ . The upper diagram shows the evolution of the state variables ( $\vartheta$  blue,  $\dot{\vartheta}$  green,  $s$  red,  $\dot{s}$  cyan). The lower diagram shows the control input evolution.

$N$	4	8	12	16	20	24
$T_c$	0.00233	0.00270	0.00306	0.00416	0.00522	0.00640

Table 1: Computation time  $T_c$  (in seconds) for different prediction horizons.

It can be noted that the transient becomes better as the planning horizon is enlarged.

Table 1 shows the computation time  $T_c$  on a processor with a base frequency of 2.3 GHz. Although a non-dedicated hardware has been used, the computation time is much smaller than  $T$ , even for large prediction horizons.

Table 2 shows the optimal cost corresponding to the initial condition  $x_0 = [0 \ 0 \ 0.5 \ 0]^\top$ , a time horizon of 2.4 s, and different values of  $\tau$  and  $N$ . By reducing  $\tau$ , better discrete-time performances ( $J_D$ ) are obtained. The continuous-time performance ( $J_C$ ), computed numerically, is not significantly better than the discrete-time performance.

As far as the constraints are concerned, by starting the system from the aforementioned initial state, the control constraint is never active during the transients. Instead, the constraints are active by starting the system from  $\mathbf{x}_0 = [0 \ 0 \ 0.75 \ 0]^\top$ , which is at a greater distance from the target (zero state), and choosing  $u_{max} = 0.5$ . The corresponding transient is shown in Figure 7 for a planning horizon  $N = 6$ .

The control law is effective in this case too and the settling time is only slightly

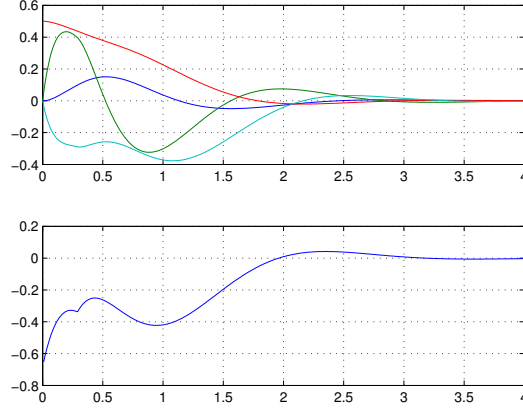


Figure 5: Simulation of the cart-pendulum behaviour starting from  $\mathbf{x}_0 = [0 \ 0 \ 0.5 \ 0]^T$  for  $\tau = 0.2 \text{ s}$  and  $N = 6$ . The upper diagram shows the evolution of the state variables ( $\vartheta$  blue,  $\dot{\vartheta}$  green,  $s$  red,  $\dot{s}$  cyan). The lower diagram shows the control input evolution.

$N$	6	12	24	40
$\tau$	0.4	0.2	0.1	0.06
$J_D$	30.23	17.90	14.72	13.85
$J_C$	29.11	16.71	14.02	13.61

Table 2: Optimal discrete-time (guaranteed) cost  $J_D$  and numerically-evaluated continuous-time cost  $J_C$ .

larger than the previous case.

## 6. Conclusions

The implementation of Model Predictive Control often becomes a “race against time” since the time to compute online the control must be smaller than the sampling time. This drawback hinders the application of MPC-based techniques fast systems, especially when the time horizon is long. The problem is even more serious when constraints are imposed on some variables.

The modified MPC technique suggested in [6] and adopted in this paper avoids these difficulties by relieving the computation of the optimal trajectory from the burden of an excessive time resolution. In fact, by exploiting the Euler Auxiliary System, the (small) sampling time and the (much larger) time parameter used

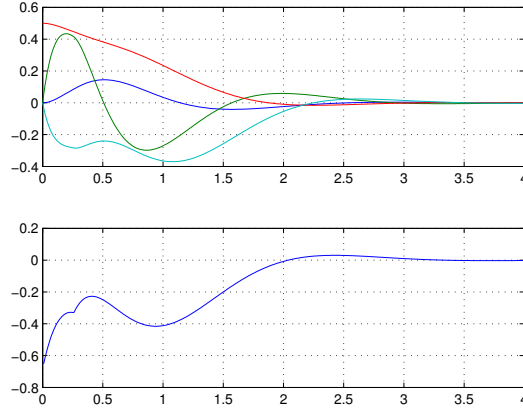


Figure 6: Simulation of the cart-pendulum behaviour starting from  $\mathbf{x}_0 = [0 \ 0 \ 0.5 \ 0]^T$  for  $\tau = 0.2 \text{ s}$  and  $N = 12$ . The upper diagram shows the evolution of the state variables ( $\vartheta$  blue,  $\dot{\vartheta}$  green,  $s$  red,  $\dot{s}$  cyan). The lower diagram shows the control input evolution.

in the optimisation problem may be kept distinct. Despite the coarser resolution for computing the control input, however, both stabilisation and constraint satisfaction are guaranteed without appreciably deteriorating the control system performance.

A new easily verifiable condition based on Lyapunov-functions theory has been provided. It ensures the robustness of the adopted approach which has been applied to the control of two fast electromechanical systems.

## References

- [1] S. Almér, S. Mariétoz, and M. Morari. Sampled data model predictive control of a voltage source inverter for reduced harmonic distortion. *IEEE Transactions on Control Systems Technology*, 21(5):1907–1915, September 2013.
- [2] D. Angeli, A. Casavola, G. Franzè, and E. Mosca. An ellipsoidal off-line MPC scheme for uncertain polytopic discrete-time systems. *Automatica*, 44(12):3113–3119, December 2008.
- [3] A. Bemporad, M. Morari, V. Dua, and E.N. Pistikopoulos. The explicit linear quadratic regulator for constrained systems. *Automatica*, 38(1):3–20, 2002.

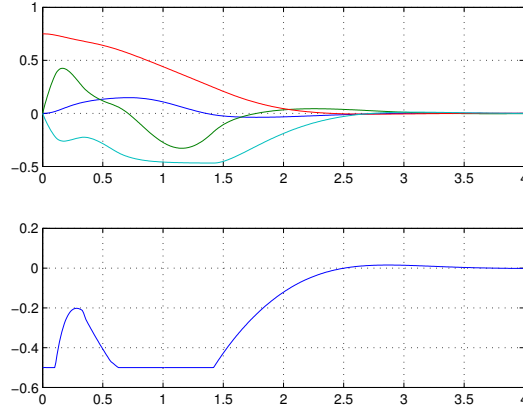


Figure 7: Simulation of the cart-pendulum behaviour starting from the initial state  $\mathbf{x}_0 = [0 \ 0 \ 0.75 \ 0]^\top$  with  $T = 0.01 \text{ s}$ ,  $\tau = 0.2 \text{ s}$  and  $u_{max} = 0.5$ . Upper diagram: state evolution. Lower diagram: control input evolution.

- [4] F. Blanchini. Set invariance in control—a survey. *Automatica*, 35(11):1747–1767, 1999.
- [5] F. Blanchini and S. Miani. *Set-theoretic methods in control*. Birkhauser, 2007.
- [6] F. Blanchini, S. Miani, and F.A. Pellegrino. Suboptimal receding horizon control for continuous-time systems. *IEEE Transactions on Automatic Control*, 48(6):1081–1086, June 2003.
- [7] F. Blanchini, S. Miani, M. Tomasini, L. Tubiana, U. Viaro, and M. Zigliotto. A minimum-time control strategy for torque tracking in permanent magnet AC motor drives. *Automatica*, 43:505–512, 2007.
- [8] S. Bolognani, S. Bolognani, L. Peretti, and M. Zigliotto. Design and implementation of model predictive control for electrical motor drives. *IEEE Transactions on Industrial Electronics*, 56(6):1925–1936, June 2009.
- [9] E.F. Camacho and C. Bordons. *Model Predictive Control*. Advanced Textbooks in Control and Signal Processing. Springer-Verlag, 2007.
- [10] A. Casavola, G. Franzè, D. Menniti, and N. Sorrentino. Voltage regulation in distribution networks in the presence of distributed generation: A volt-

- age set-point reconfiguration approach. *Electric Power Systems Research*, 81(1):25–34, June 2011.
- [11] P.D. Christofides, J. Liu, and D. Muñoz de la Peña. *Networked and distributed predictive control: Methods and nonlinear process network applications*. Advances in Industrial Control Series. Springer-Verlag, 2011.
- [12] T. Geyer, G. Papafotiou, and M. Morari. Model predictive direct torque control-part i: Concept, algorithm, and analysis. *IEEE Transactions on Industrial Electronics*, 56(6):1894–1905, June 2009.
- [13] T. Geyer and D.E. Quevedo. Multistep finite control set model predictive control for power electronics. *IEEE Transactions on Power Electronics*, 29(12):6836–6846, December 2014.
- [14] G. C. Goodwin, M. M. Seron, and J. A. De Doná. *Constrained control and estimation: an optimisation approach*. Springer, 2006.
- [15] R. Kennel, A. Linder, and M. Linke. Generalized predictive control (GPC)-ready for use in drive applications? In *Proceedings of the IEEE PESC*, pages 1839–1844, 2001.
- [16] S. Kouro, P. Cortés, R. Vargas, U. Ammann, and J. Rodríguez. Model predictive control—A simple and powerful method to control power converters. *IEEE Transactions on Industrial Electronics*, 56(6):1826–1838, June 2009.
- [17] A. Linder and R. Kennel. Model predictive control for electrical drives. In *Proceedings of the IEEE PESC*, pages 1793–1799, Recife, Brazil, 2005.
- [18] S. Mariéthoz and A. Domahidi M. Morari. High-bandwidth explicit model predictive control of electrical drives. *IEEE Transactions on Industry Applications*, 48(6):1980–1992, November/December 2012.
- [19] D. Q. Mayne, J.B. Rawlings, C.V. Rao, and P.O.M. Scokaert. Constrained model predictive control : stability and optimality. *Automatica*, 36:789–814, 2000.
- [20] S.J. Qin and T.A. Badgwell. An overview of nonlinear model predictive control applications. In *Nonlinear model predictive control*, pages 369–392. Springer-Verlag, 2000.

- [21] S.J. Qin and T.A. Badgwell. A survey of industrial model predictive control technology. *Control Engineering Practice*, 11(7):733–764, 2003.
- [22] S. Richter, S. Mariéthoz, and M. Morari. High-speed online MPC based on a fast gradient method applied to power converter control. *Proc. of the American Control Conference*, pages 4737–4743, 2010.
- [23] J. Rodriguez and P. Cortés. *Predictive Control of Power Converters and Electrical Drives*. Wiley-IEEE, 2012.
- [24] D. Schindele and H. Aschemann. Fast nonlinear MPC for an overhead travelling crane. *Proc. of the IFAC World Congress*, 48(277:2013):1–12, 2011.
- [25] M. Sznaier and M. J. Damborg. Suboptimal control of linear systems with state and control inequality constraint. In *Proceedings of the 26th Conference on Decision and Control, Los Angeles, CA*, pages 761–762, 1987.
- [26] Z. Wan and M.V. Kothare. An efficient off-line formulation of robust model predictive control using linear matrix inequalities. *Automatica*, 39:837–846, 2003.
- [27] Y. Wang and S. Boyd. Fast model predictive control using online optimization. *IEEE Transactions on Control Systems Technology*, 18(2):267–278, March 2010.
- [28] T.-C. Wee, A. Astolfi, and X. Ming. The design and control of a bipedal robot with sensory feedback. *Int. J. Adv. Robotic Sy.*, 10:7963–7968, 2013.
- [29] Y. Xie, R. Ghaemi, J. Sun, and J.S. Freudenberg. Model predictive control for a full bridge DC/DC converter. *IEEE Transactions on Control Systems Technology*, 20(1):164–172, January 2012.

### **Proof of Proposition 1**

To complete the proof, points in which  $\Psi_N^{(\tau)}$  is not differentiable need to be considered. Since the system is linear,  $\Psi_N^{(\tau)}$  is positive-definite and convex. Hence, by defining the subgradient of a function  $g$  at  $x$  as the set

$$\partial g(x) \triangleq \{z \in \mathbb{R}^n : g(y) - g(x) \geq z^\top (y - x), \text{ for all } y \in \mathbb{R}^n\},$$

the directional derivative of  $\Psi$  in the direction  $y$  is given by (for details see, e.g., [5])

$$\lim_{h \rightarrow 0^+} \frac{\Psi(x + hy) - \Psi(x)}{h} = \sup_{z \in \partial\Psi(x)} z^\top y.$$

(Note that, at any point in which  $\Psi$  is differentiable, the subgradient is a singleton equal to the gradient.)

Then, considering the directional derivative of  $\Psi_N^{(\tau)}$  along the trajectories of (24), we have

$$\begin{aligned} D^+ \Psi_N^{(\tau)}(x) &= \lim_{h \rightarrow 0^+} \frac{\Psi_N^{(\tau)}(x + h(Ax + Bu) + h\Delta(x)x) - \Psi_N^{(\tau)}(x)}{h} \\ &= \sup_{z \in \partial\Psi_N^{(\tau)}(x)} z^\top (Ax + Bu + \Delta(x)x) \\ &\leq \sup_{z \in \partial\Psi_N^{(\tau)}(x)} z^\top (Ax + Bu) + \sup_{z \in \partial\Psi_N^{(\tau)}(x)} z^\top \Delta(x)x \\ &\leq -\phi(x) + \lim_{h \rightarrow 0^+} \frac{\Psi_N^{(\tau)}(x + h\Delta(x)x) - \Psi_N^{(\tau)}(x)}{h} \\ &= -\phi(x) + \psi(x) < 0. \end{aligned}$$